



## Effect of Lowering Tube Potential and Increase Iodine Concentration of Contrast Medium on Radiation Dose and Image Quality in Computed Tomography Pulmonary Angiography Procedure: A Phantom Study

Justin E Ngaile<sup>1,2\*</sup>, Peter K Msaki<sup>2</sup>, Evarist M Kahuluda<sup>1</sup>, Furaha M Chuma<sup>1</sup>, Jerome M Mwimanzi<sup>1</sup> and Ahmed M Jusabani<sup>3</sup>

<sup>1</sup> Radiation Control Directorate, Tanzania Atomic Energy Commission, PO Box 743, Arusha, Tanzania.

<sup>2</sup> Department of Physics, University of Dar es Salaam, PO Box 35063, Dar es Salaam, Tanzania.

<sup>3</sup> The Agha Khan Hospital, PO Box 2289, Dar es Salaam, Tanzania.

\*Corresponding author, E-mail: justine.ngaile@taec.go.tz; jngaile@gmail.com

Received 31 Jan 2021, Revised 2 Aug 2021, Accepted 4 Aug 2021, Published Aug 2021

DOI: <https://dx.doi.org/10.4314/tjs.v47i3.29>

### Abstract

The aim of the study was to examine the effect of lowering tube potential and increase iodine concentration on image quality and radiation dose in computed tomography pulmonary angiography procedure. The pulmonary arteries were simulated by three syringes. The syringes were filled with 1:10 diluted solutions of 300 mg, 350 mg and 370 mg of iodine per millilitre concentration in three water-filled phantoms simulating thin, intermediate and thick patients. The phantoms were scanned at 80 kVp, 110 kVp and 130 kVp and 0.6 second rotation time using a 16 slice computed tomography (CT) scanner. The tube current was either fixed at 80, 100, 200, 250 and 300 mA or automatically adjusted with quality reference tube current-time product (mAs<sub>QR</sub>). In comparison with 130 kVp, images acquired at 80 kVp and 110 kVp, respectively, showed 76.2% to 99% and 19% to 26% enhancement in CT attenuation of iodinated contrast material. A volume CT dose index (CTDI<sub>vol</sub>) reduction by 35.3% was attained in small phantom with the use of 80 kVp, while in the medium phantom, a CTDI<sub>vol</sub> reduction by 29.9% was attained with the use of 110 kVp instead of 130 kVp. In light of the above, lowering tube potential and increase iodinated CM could substantially reduce the dose to small-sized adults and children.

**Keywords:** Angiography, Computed tomography, Low tube potential, Iodinated contrast medium, Radiation dose.

### Introduction

Computed tomography pulmonary angiography (CTPA) procedure is a well-established minimally invasive imaging technique for diagnosing and evaluating acute pulmonary embolism (Björkdahl and Nyman 2010, Hu et al. 2017, Ma et al. 2017). The diagnostic values of the CTPA procedures have been substantially improved with the use of advanced multi-detector computed tomography (MDCT) techniques owing to its improved

spatial and temporal resolutions (Moynihan et al. 2017). However, despite the potential advantage and promising clinical results, CTPA procedures suffer from unavoidable high doses delivered to individual patients. As a result of the high doses to patients associated with this procedure, there have been concerns of the possible undesired health effects such as stochastic cancer risks and deterministic risks of radiation injuries (Sun and Ng 2010, Aschoff et al. 2017). The great concerns are the

young patients and in women in child bearing age who are at high risk of carcinogenesis from diagnostic radiation (Moynihan et al. 2017).

These concerns have prompted the need for appropriate strategies to minimize radiation doses to patients from MDCT angiography procedures, using imaging parameters to optimize dose and image quality (Hausleiter et al. 2009). Strategies or methods that can be employed to lower radiation doses to patients undertaking MDCT angiography procedures have been well established (Sun and Ng 2010, Goo 2012). These strategies may include automatic tube current modulation (ATCM), iterative reconstruction algorithms, X-ray tube loading (pitch-corrected milliampere seconds,  $mAs_{eff}$ ), pitch, scan length, and choice of reconstruction algorithms (Björkdahl and Nyman 2010, Goo 2012, Hu et al. 2017).

A number of studies have shown that lowering tube potential based on patient weight, size and age at constant iodinated contrast medium (CM) could minimize radiation doses to patients by as much as 50% without loss of diagnostic image quality (Björkdahl and Nyman 2010, Moynihan et al. 2017, Hu et al. 2017). It is desired that dose could further be reduced by lowering kVp and increase concentrations of CM based on patient size. Although preceding scientific publications have reported that a reduction in kVp is associated with an increase in image contrast, to the best of our knowledge, only few studies have been conducted to examine the effects of lowering tube voltage and increase concentration of CM based on patient size (Nyman et al. 2012, Papadakis et al. 2013, Razak et al. 2013). Thus, the aim of this study was to examine the effect of lowering the tube potential and increase concentration of CM on image quality and radiation dose in CTPA procedure of various patient sizes.

## **Materials and Methods**

### **Description of data sources**

The data used in the present phantom study were collected from the Besta Diagnostic Centre (BDC), in Dar es Salaam, Tanzania.

The BDC is equipped with Siemens Somatom Emotion 16 (Siemens Shanghai Medical Equipment Limited, Shanghai, China) manufactured in 2013 and installed in 2014. The CT scanner is equipped with axial and helical modes with solid state array detector (Siemens UFC). The focal spot to iso-centre distance and focal spot-to-detector distance for the Somatom Emotion 16 are 535 and 940 mm, respectively. The total X-ray beam filtration including contributions from permanent filtration and inherent filtration amounts to 3.6 mm Al equivalent. The scanning parameters employed by the BDC for CTPA procedures were configuration of 16 (detectors) x 1.2 mm (detector collimation), rotation time of 0.6 second, section thickness of 5.0 mm, section interval of 5.0 mm, table speed of 12 mm, scan field of view (FOV) of 235 mm, reconstruction algorithm (kernel) B41s medium and pixel matrix size of 512 x 512. Prior to the use of the CT scanner for phantom studies, the performance characteristics, such as kVp reproducibility and accuracy, were performed in compliance with existing standards (IPEM 2005) using Unfors Xi multimeter (Unfors Xi, Ser. No. 181017, Unfors Inc., Billdal, Sweden). The output reproducibility, linearity and half-value layer (HVL) measurements were performed using a pencil shaped ionization chamber (Unfors Xi, Ser. No. 177013, Unfors Inc., Billdal, Sweden) that has calibration traceable to Swedish National Testing and Research Institute. The image quality tests including CT image noise, CT number accuracy and CT number uniformity were performed using a CT performance phantom (Victoreen, model 76-410-4130, Invasion, and Nuclear Associate, New York, USA). Prior to the study, ethical clearance was obtained from the National Institute for Medical Research.

### **Phantom study**

The main incentive of the phantom study was to investigate the relative change in attenuation and image noise at various tube potentials to be able to calculate the relative change in contrast-to-noise ratio (CNR)

between 80 kVp and 130 kVp. In order to achieve the objective of this study, three different rectangular water containers, which simulated a small-sized (thin) (150 mm x 300 mm x 300 mm), medium-sized (200 mm x 300 mm x 300 mm), and large-sized (240 mm x 300 mm x 300 mm) patient were fabricated using about 10 mm thick Perspex Trademark acrylic sheet.

In each water-filled phantom three 65 ml syringes of 30 mm diameter simulating contrast enhanced segmental pulmonary arteries were inserted at the iso-centre of the phantom, as shown in Figure 1. These syringes were filled carefully with 1:10 dilution of CM and distilled water, simulating contrasted blood in the vessels, and sealed. For the syringe on the left side, the diluted solution of iodine concentration of 300 mg of iodine (mgI) per millilitre (Utravist 300, Berlin, Germany) was used, while for the syringe on the middle, iodine concentration of 350 mg of iodine per millilitre (Omnipaque 350, GE healthcare Ireland, Cork, Ireland) was used and for the syringe on the right side, the iopamidol iodine concentration of 370 mg of iodine per millilitre (Pamidol 370, Unique Pharmaceutical Labs, Dist-Bharuch, India) was placed.



**Figure 1:** Typical irradiation set up of the phantom.

### Scanning technique

The water-filled chest phantom was positioned within the iso-centre of the CT scanner, with cross section perpendicular to the scanner's z-axis, as shown in Figure 1. The

phantoms were scanned with a 16-section MDCT scanner using two sets of scanning parameters. Regardless of the kVp and mA, the phantoms were scanned at the same table position using rotation time of 0.6 second, section thickness of 5.0 mm, section interval of 5.0 mm, table speed of 12 mm. Scanning was further performed with 1.2 mm (detector collimation), standard reconstruction algorithm (kernel) of B41s medium, large scanning field of view (FOV) with display FOV of 235 mm and pixel matrix size of 512 x 512. In the first set of experiments, the water-filled phantoms were scanned each time with 80, 110 and 130 kVp using fixed tube current technique at 80, 100, 200, 250 and 300 mA. In the second set of experiments, the phantoms were scanned each time with 80 kVp, 110 kVp and 130 kVp at quality reference tube current-time product ( $mAs_{QR}$ ) values ranged from a minimum of 50  $mAs_{QR}$  to a maximum of 300  $mAs_{QR}$  using the automatic dose modulation protocols provided by the manufacturer (CAREdose4D, Siemens Medical Systems). This modulation technique adjusts CT mA in a real time manner both in the xy-plane and the longitudinal z-axis to keep the image quality at an optimal level. Effective mAs values were averaged on the reconstructed 5 mm thick transverse slices of the first series and referred as the optimized mAs value (100%) for the given kVp and phantom size setting.

### Measurements of CT attenuation, images noise and contrast-to-noise ratio

The CT attenuation value (Hounsfield unit; HU) and its standard deviation (SD) of CM in each syringe and of the water phantom were determined by placing a circular region of interest (ROI) (of an area of  $100 \text{ mm}^2$ ) at the middle of the syringe, as shown in Figure 2. From the Figure 2, the left syringe corresponded to 300 mg I/mL, middle syringe corresponded to 350 mg I/mL and left syringe corresponded to 370 mg I/mL. The measurements were obtained in the three phantom sizes acquired with three tube potentials. To minimize measurement errors,

each parameter was measured five times on 5 consecutive images. Image noise was defined as the average of the SDs of the CT attenuation values measured in a homogeneous central location of the phantom (Moynihan et al. 2017). Contrast to noise ratio (CNR) was used as an objective parameter to characterize image quality. The CNR on each set of images was obtained using Equation 1 (Gupta et al. 2003, Schindera et al. 2013):

$$CNR = \frac{(ROI_m - ROI_b)}{SD_b} \quad (1)$$

where  $ROI_m$  and  $ROI_b$  are the CT attenuation values of the low-contrast objects in a 30 mm diameter region of interest and of the background region of interest, respectively.  $SD_b$  is the standard deviation of the attenuation of the background. The relative change in image noise when reducing tube potential from 130 kVp to 80 kVp was then compared with the theoretical changes according to Nagel et al. (2002), which is inversely proportional to the square root of the quote between the final (80 kVp) and initial tube potential (130 kVp) to the power of 3.5, i.e.,

$$1/\sqrt{(80/130)^{3.5}} = 2.34, \quad \text{i.e.} \quad 134\% \text{ increase.}$$



**Figure 2:** A cross sectional CT image of contrast phantom containing three syringes of 65 mL in volume that have been filled with different concentrations of iodinated of 300, 350 and 370 mg of iodine/mL CM.

#### Measurement of radiation dose and determination of figure of merit

In order to estimate the patient dose, the volume CT dose index ( $CTDI_{vol}$ ) generated by

the CT scanner system was employed.  $CTDI_{vol}$  is a standardized for a 32 cm diameter acrylic phantom and, therefore, does not depend upon patient size if the tube parameters are left unchanged. In the present study, exposure setting (mAs) was modulated according to the phantom size; with the intention that the use of  $CTDI_{vol}$  to characterize exposure at various phantom sizes was conceivable. To determine the percentage dose reduction (% DR) achieved, when a lower than the 130 kVp was employed in automatic exposure control, Equation 2 was applied (Papadakis et al. 2013):

$$\%DR = \frac{[(CTDI_{vol})_{mAs_{QR}}^{130kV} - (CTDI_{vol})_{mAs_{mod}}]}{(CTDI_{vol})_{mAs_{QR}}^{130kV}} \times 100 \quad (2)$$

where  $(CTDI_{vol})_{mAs_{QR}}^{130kV}$  is the  $CTDI_{vol}$  at 130 kV and  $mAs_{QR}$  settings, which are prescribed by the routine thorax examination protocols,  $(CTDI_{vol})_{mAs_{mod}}$  is the  $CTDI_{vol}$  at a given kVp and  $mAs_{mod}$  value, which produce images of similar image noise as that at the images produced using the routine exposure parameters. The relative change in  $CTDI_{vol}$  when decreasing applied tube potential from 130 to 80 kVp was then compared with the theoretical changes according to Nagel et al. (2002), which state that radiation doses to patients vary with the quote between the final (80 kVp) and initial tube potential (130 kVp) to the power of 2.5, i.e.,  $(80/130)^{2.5} = 0.30$ , i.e. 70% decrease. In order to examine the influence of applied tube potential and phantom size on the CNR in relation to radiation dose to patient,  $CNR^2/CTDI_{vol}$  was calculated as figure of merit (FOM) for each setting. By definition, FOM is independent of exposure and can be used as a measure of improvement in image quality per exposure risk to patient (Szucs- Farkas et al. 2008).

## Results and Discussions

### Performance characteristics of CT scanner

The results of the basic performance characteristics of the scanner are summarized in Table 1.

**Table 1:** Basic performance characteristics of CT scanner employed in the study

Parameter	Measured	Tolerance limit
kV accuracy (%)	-4.5	±10
kV reproducibility (%)	0.8	5
Exposure time reproducibility (%)	0.9	5
Output reproducibility (%)	0.2	5
Output linearity (mGy mAs <sup>-1</sup> ) (%)	0.9	10
HVL, mmAl (at 130 kV)	11	>3.5
CT number accuracy	0.8 HU	±5 HU
CT image noise	10.4 HU	
CT spatial number uniformity	2.7 HU	±5 HU

**CT attenuations of contrast media dilutions**

The CT attenuation was measured as described earlier using the ROI software available from the scanner by employment of two sets of exposure parameters for different phantom sizes. The relationship between the mean values of CT attenuation of 1:10 dilutions of 300 mg, 350 mg and 370 mg of iodine per milliliter of CM with different kVp for three different phantom sizes (S: small; M: medium; L: large) are given in Figure 3. It is important to note from the Figure 3 that if other parameters such as mAs (i.e., 300 mAs) are kept constant, a reduction in kVp had substantial improvement in mean CT attenuation values with constant phantom size and iodinated CM. However, the level of increase in CT attenuation owing to lowering of the kVp was slightly higher in small phantom than in the larger ones. For instance, lowering of the kVp from the recommended 130 kVp to 110 kVp for the large phantom at constant concentration of 300 mgI/mL resulted in an improved mean CT attenuation by 24% [(656.1–528.2 HU)/528.2 HU], while for the small phantom, the mean CT attenuation increased by 26% [(689.4–545.9 HU)/545.9 HU]. Further reduction of the kVp from 130 kVp to 80 kVp for the large phantom resulted in an increase in mean CT attenuation by 86% [(982.9–528.2 HU)/528.2 HU], while for the small phantom, the mean CT attenuation increased by 99% [(1089–545.9 HU)/545.9

HU]. The larger mean CT attenuation of iodine CM observed in the small phantom than large phantoms was mainly explained by the fact that there is an increased beam hardening of the X-rays photons in the large phantom relative to the small phantom (Schindera et al. 2010, Ngaile et al. 2012, Razak et al. 2013).

On the other hand, the results presented in the Figure 3 further demonstrate that there is a considerable decrease in mean CT attenuation of iodine CM with increasing phantom size at all the three kVp settings. This results in an increase in the energy of the X-ray beam, which, in turn, leads to a lower the CT attenuation of the iodinated CM for the large phantom owing to lower photoelectric effects and increased Compton scattering (Schindera et al. 2010, Papadakis et al. 2013). It is further evident from Figure 3 that the mean CT attenuation value in the diluted 370 mg iodine/mL CM (HU<sub>370</sub>) was significantly ( $p < 0.001$ ) higher than in the dilution of 350 mg iodine/mL CM (HU<sub>350</sub>), and 300 mg iodine/mL CM (HU<sub>300</sub>) in every setting. For instance, lowering of kVp from 130 to 80 for the 300 mg iodine/mL (at constant phantom size and fixed mAs) resulted in an increase in mean CT attenuation values by 86.1 % [(982.9–528.2 HU)/528.2 HU], while for the 370 mg iodine/mL, the mean CT attenuation value increased by 92.5% [(1179.4–612.6 HU)/612.6 HU].

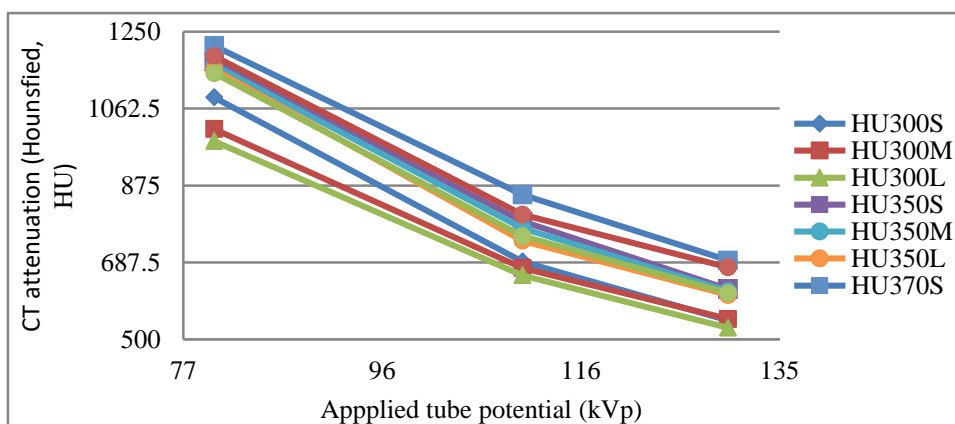


**Figure 3:** CT attenuation values of 1:10 dilutions of 300, 350 and 370 mg iodine/mL contrast media (HU<sub>300</sub>, HU<sub>350</sub>, and HU<sub>370</sub>, respectively) at different kVp values and phantom size settings.

Measurements at all kVp settings revealed that CT attenuation followed a decreasing trend for all three CMs when the phantom was changed from small to large. Further it was observed that the reduction in kVp had a superior effect on the CT attenuation values of the region enhanced with iodinated CM than it had on the CT attenuation values of non-enhanced regions. In order to investigate the influence of the CM concentration on CT attenuation value, the correlation between CT attenuation values with CM concentration for different kVp (at medium phantom size and 100 mAs<sub>QR</sub>) was performed using linear regression.

The results of the linear regression analysis between the mean values of CT attenuation and different concentrations of iodinated CM at 80 kVp, 110 kVp and 130 kVp are shown in Figure 4. It is marked from the Figure 4 that there is very strong positive correlation between the mean values of CT attenuation of each of the three syringes with increased iodine concentrations ( $r = 0.996-1.0$ ,  $p < 0.001$ ) for all three kVps, with the CM concentration accounting up to 100% of the CT attenuation variations. Higher CT attenuation values were obtained at 80 kVp than at 110 kVp and 130 kVp at medium phantom and 100 mAs<sub>QR</sub>.

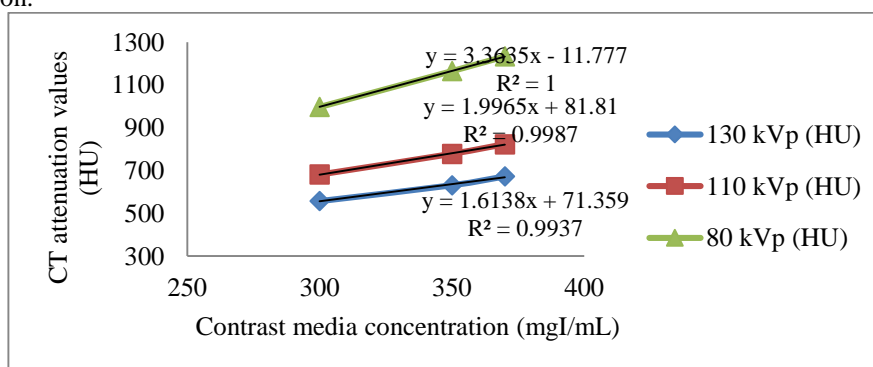


**Figure 4:** The mean CT attenuation values of syringes of the phantom that were scanned at 130 kVp, 110 kVp and 80 kVp increased with increasing iodine concentrations.

The mean CT attenuation of the syringes of the phantom increased with increasing iodine concentrations; the increase was higher at 80 kVp than it was at 110 kVp and 130 kVp. This phenomenon is largely explained by the fact that at a lower tube potential, the influence of the photoelectric interaction is greater compared with Compton scattering effects because of the 33-keV k-edge of iodine (Nagel et al. 2002). It is further evident from the Figure 4 that the slope of the line with 80 kVp was 1.7 and 2.1 higher than lines for 110 kVp and 130 kVp, respectively.

#### CT image noise

The relationship between the mean values of image noise and kVp at constant

milliamperere seconds (i.e. 250 mAs<sub>QR</sub>) is shown in Figure 5. It is worth to note from the figure that through lowering the kVp at a constant phantom size, there was a considerable increase in image noise in the resulted images. One possible explanation for this phenomenon is that the images acquired using lower kVp tend to be much noisier owing to higher absorption of lower energy photons by the patient (Schindera et al. 2013, Hu et al. 2017). Another possible explanation for this phenomenon is that in this low-dose range, there are considerable photon-starving artifacts owing to the decreased penetration capability of the lower energy photons and electronic noise, which originates from the X-ray detector system (Szucs-Farkas et al. 2008).

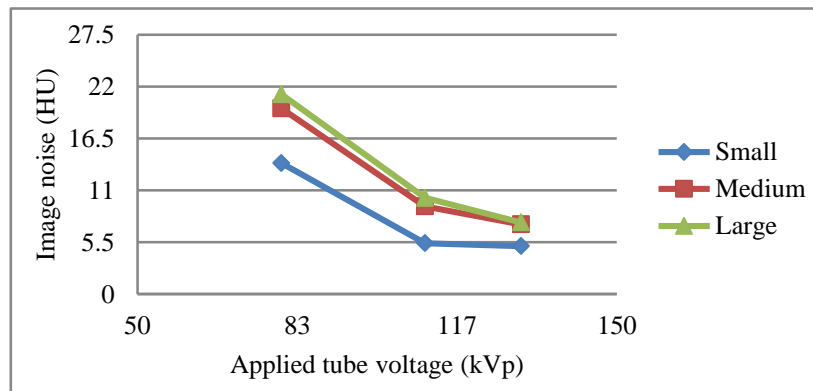


**Figure 5:** Image noise as a function of the applied tube voltage.

On the other hand, it was revealed from the results presented in Figure 5 that the level of image noise was less for the smaller phantom than in the larger phantoms. For example, lowering the tube potential from 130 kVp to 80 kVp for the large phantom at 250 mAs<sub>QR</sub> resulted in an increase in image noise by 180.3% [(21.2–7.6 HU)/7.6 HU], while for the small phantom, the image noise increased by 172.5% [(13.9–5.1 HU)/5.1 HU]. The mean image noise increased more in the large phantom (180%) compared with the theory (Nagel et al. 2002) when lowering the tube potential from 130 kVp to 80 kVp. The observed high image noise in the large phantom could be attributed to large

absorption, scatter radiation and electronic noise. The slightly decrease of image noise observed for the small-sized phantom relative to the large ones was largely explained by the fact that there is less intervening material to attenuate the photons for the small phantom compared to the large phantoms; as a result, a considerable number of photons is transmitted to the detector. These findings have an implication for the small-sized adult and children patients that undergo CTPA procedures. This is mainly because for the small-sized adult and children CT angiography procedures, the minimization of scanning parameters does not significantly affect the image quality as does to the large adult patient.

The relationship between the image noise variations and  $mAs_{QR}$  for three different phantom sizes at constant tube potential of 110 kVp is given in Figure 6. As anticipated, it is demonstrated from the Figure 6 that image noise decreases with increase of  $mAs_{QR}$ . For instance, for the small-sized phantom, images obtained at different  $mAs_{QR}$  have almost the same image noise levels, with slightly higher image noise for images acquired at 50  $mAs_{QR}$ . However, with increase of the phantom size, the lower  $mAs_{QR}$  yield images with higher image noise level relative to images obtained at higher  $mAs_{QR}$ . For instance, reduction of  $mAs_{QR}$  from 250 to 50 for the large phantom, resulted to an increase in image noise by 134% [(23.9–10.2 HU)/10.2 HU], while for the small phantom, the image noise increased by 117% [(11.7–5.4 HU)/5.4 HU]. The considerable increase in image noise observed for the large phantom relative to the small phantom is due to the fact that large phantom experiences more absorption and scattering owing to large cross-sectional area to the X-ray beam; as a result,

few photons reach the detector. The results presented in the Figure 6 further revealed that there is a substantial variation in image noise among different phantom sizes when the  $mAs_{QR}$  settings proposed by the MDCT system application guide are selected. In the present study, it was presumed that images of adequate diagnostic quality are attained on large-sized phantom when scanned with the standard scanning parameters, that is, 130 kVp and  $mAs_{QR}$  of 150. The image noise measured for the large phantom was 13.0 HU. To maintain the same image noise level among the small and medium phantoms, the  $mAs_{QR}$  setting should be reduced from 150 to less than 50 for the small phantom and 135 for the medium phantom. By matching the image noise considered acceptable for the standard phantom, there was a 10% [(150–135  $mAs_{QR}$ )/150  $mAs_{QR}$ ] decrease in the  $mAs_{QR}$  value for the medium phantom and a 67% [(150–50  $mAs_{QR}$ )/150  $mAs_{QR}$ ] decrease in the  $mAs_{QR}$  value for the small phantom.

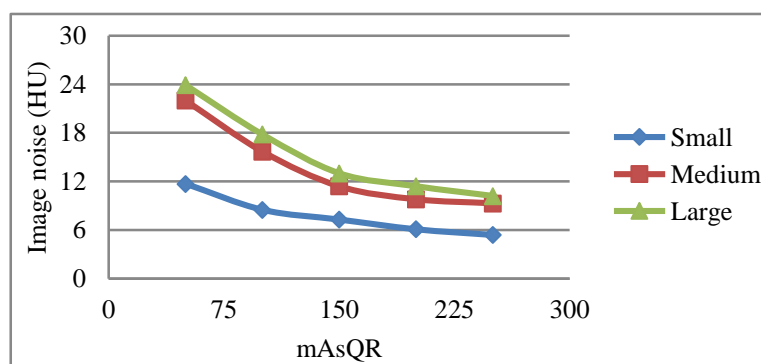


**Figure 6:** Image noise varied as function of  $mAs_{QR}$  for each phantom at 110 kVp.

The observed significant reduction in the  $mAs_{QR}$  for the small phantom was largely attributed to the fact that X-ray photons have higher penetration to the smaller phantom than larger phantom owing to less attenuation instigated by intervening materials. These findings have implications for medium and small-sized adult and children patients that undergo clinical CT angiography procedures.

On the other hand, it was revealed from Figure 6 that the measured image noise was equal to  $a(mAs_{QR})^b$ , where  $a$  is a constant unique to the phantom size and tube potential (Ngaile et al. 2012). This equation yields straight lines with slope  $b$  when perceived in log-log axes. The best-fit parameters and regression coefficient ( $R^2$ ) per phantom size are shown in Table 2.

**Table 2:** Fit parameters of the relationship between the image noise and  $mas_{er}$  [ $Y = a(mas_{er})^b$ ]

Phantom size	$a$	$b$	$R^2$
Small phantom (15 cm depth)	76.43	-0.47	0.999
Medium phantom (20 cm depth)	201.5	-0.56	0.986
Large phantom (24 cm depth)	206.2	-0.54	0.989

It is noticeable from Table 2 that the slope of the line for the small phantom was approximately -0.5, which is Poisson statistics for X-rays (i.e., noise  $\propto$  dose<sup>-0.5</sup>) (Szucs-Farkas et al. 2008). It is further noticeable from the table that slopes for the medium and large phantoms were relatively higher in magnitude than for the small phantom. This might be attributed to the scattered radiation and other

sources of noise in a photon-starving environment as observed elsewhere (Ngaile et al. 2012).

#### Contrast to noise ratio

Table 3 shows the calculated CNR at different applied kVp, phantom sizes and concentrations of CM.

**Table 3:** CT attenuation values (HU) and CNR at different contrast media at 80 and 110 kVp compared with 130 kVp at 250 mAs<sub>OR</sub> (Automatic selection)

Contrast Media	At 130 kVp		At 110 kVp		At 80 kVp	
	Mean CTA (HU)	CNR	Mean CTA (HU)	CNR	Mean CTA (HU)	CNR
Small phantom						
I-300	553.9	79.6	673.8 (122%)	79.4 (100%)	997.3 (180%)	73.3 (92%)
I-350	645.3	86.5	785.0 (122%)	85.7 (99%)	1159.6 (180%)	81.0 (94%)
I-370	683.8	96.1	829.2 (121%)	93.5 (97%)	1226.0 (179%)	84.9 (88%)
Medium phantom						
I-300	557.4	78.6	681.3 (122%)	76.0 (97%)	1021.4 (183%)	59.7 (76%)
I-350	631.1	84.2	777.3 (123%)	81.3 (97%)	1164.0 (184%)	68.4 (81%)
I-370	673.0	89.7	823.5 (122%)	84.0 (94%)	1229.9 (183%)	72.1 (80%)
Large phantom						
I-300	545.7	75.6	669.5 (123%)	72.8 (96%)	1008.4 (185%)	55.6 (73%)
I-350	628.6	74.1	773.0 (123%)	75.7 (102%)	1168.0 (186%)	61.3 (83%)
I-370	649.1	77.6	784.7 (121%)	76.0 (98%)	1183.2 (182%)	62.4 (80%)

Mean CTA; Mean CT attenuation (HU).

\*The percentage values in the bracket represent the percentage change of the CT attenuation values and CNR of the syringe filled with diluted CM when lowering the tube potential from 130 kVp to 110 kVp and 80 kVp.

It is marked from the table that there is a decrease of CNR as kVp decreases. For example, lowering of kVp from 130 kVp to 110 kVp for the 300 mg iodine/mL and small phantom resulted in a decrease in mean values of CNR by 0.3% [(79.4–79.6)/79.6]. Further reduction of the tube potential to 80 kVp, resulted in decrease of mean values of CNR by 7.9% [(73.3–79.6)/79.6]. In case of the large-

sized phantom, lowering of the tube potential from 130 kVp to 80 kVp for 300 mg iodine/mL, resulted in decrease of the mean values of CNR by 26.5% [(55.6–75.6)/75.6]. It is also noticeably from the Table 3 that the calculated CNR value in the diluted 370 mg iodine/mL CM (CNR<sub>370</sub>) was significantly ( $p < 0.001$ ) higher than in the dilution of 350 mg iodine/mL CM (CNR<sub>350</sub>), and 300 mg

iodine/mL CM (CNR<sub>300</sub>) for small and medium size phantoms and tube potentials of 80 kVp and 110 kVp.

The relationship between CNR and mAs<sub>QR</sub> for the three phantom sizes is shown in Figure 7. It is evident from the figure that there is a very strong positive correlation between the CNR and mAs<sub>QR</sub> ( $r = 0.998-0.999$ ,  $p < 0.001$ ) for all three phantom sizes. The relationship between CNR and mAs<sub>QR</sub> was as follows: for the small phantom,  $y$  (CNR) =  $0.170 x$  (mAs<sub>QR</sub>) + 37.28 ( $r = 0.998$ ,  $p < 0.001$ ); for the medium phantom,  $y$  (CNR) =  $0.197 x$  (mAs<sub>QR</sub>) + 27.67

( $r = 0.998$ ,  $p < 0.001$ ); and for the large phantom,  $y$  (CNR) =  $0.197 x$  (mAs<sub>QR</sub>) + 23.31 ( $r = 0.999$ ,  $p < 0.001$ ). It is also evident from the Figure 7 that the CNR is higher for the small phantom than the large one. For instance, at the standard mAs<sub>QR</sub> setting of 150, the CNR increased from 53.6 for the large phantom, to 57.2 for the medium phantom and 62.8 for the small phantom, while for 250 mAs<sub>QR</sub>, the CNR increased from 72.8 for the large phantom, to 76.4 for the medium phantom and 79.4 for the small phantom.

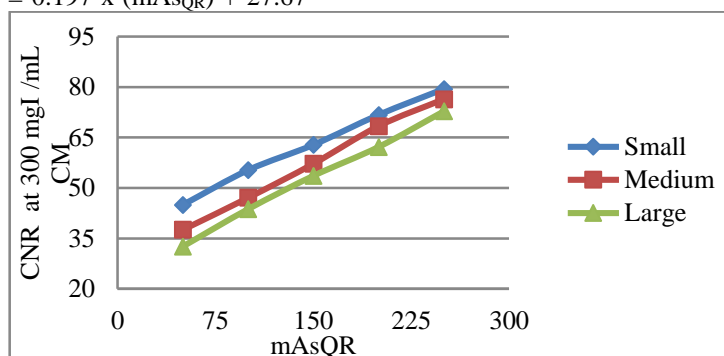


**Figure 7:** Contrast-to-noise ratio varied as function of mAs<sub>QR</sub> for each phantom.

**Figure of merit**

The relationship between the FOM and kVp at three different phantom sizes and three contrast materials is given in Figure 8. It is evident from the Figure 8 that there are very strong negative correlations between the FOM and kVp in the small-sized phantom ( $r = -0.992$  to  $-0.994$ ,  $p < 0.04$ ). This confirms that a contrast gain is attained when kVp is reduced. For the medium and large phantoms, no significant correlation between FOM and kVp was found ( $p = 0.07$  to  $0.87$ ). It is noticeably from the Figure 8 that FOM was relatively higher in the small phantom compared with the medium or large phantoms at tube potentials of 80 kVp and 110 kVp. It is also demonstrated from the Figure 8 that FOM decreases sharply with increasing kVp in the small phantom. Similar experience has been observed elsewhere (Szucs-Farkas et al. 2008). That is, in the small-sized patient, for a given mAs

value, the increase in the kVp that relates to an increase in patient dose, minimizes the FOM and hence provides a suboptimal proportion between patient dose and image quality. In the medium-sized patient, the FOM reduction with increase in kVp is less significant, while for the large-sized phantom, no significant variation of FOM was observed. This finding substantiates that for the MDCT system employed in this study, there is no benefit on image quality with the use of 80 or 110 kVp instead of 130 kVp in large patients. In other words, minimization of dose by means of lowering the kVp will result in images with lower CNR in the large patients or obese patients. The FOM was also substantially higher for the 370 mg iodine /mL CM compared with lower concentrations of 300 and 350 mg iodine/mL CM, indicating an increase in image quality for the same CTDI<sub>vol</sub>, especially at low kVp. At higher kVp, the benefits from higher concentration decrease.

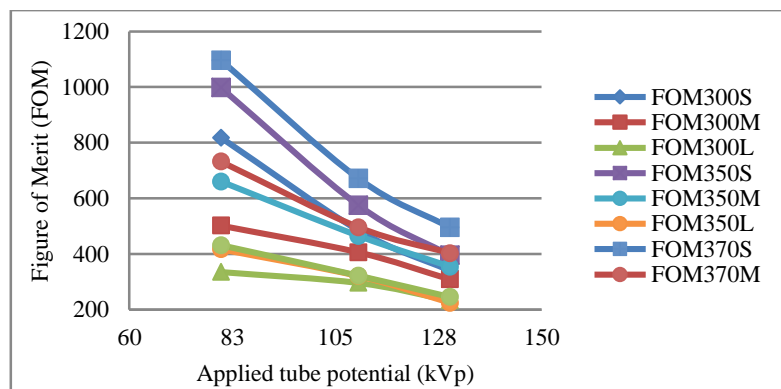


**Figure 8:** Figure of merit as function of tube potential for different phantom sizes and CM.

**Dose estimation and the automatic exposure control-based radiation dose reduction**

The results of the mean values of CT attenuation, image noise and  $CTDI_{vol}$  obtained at each set of automatic exposure control (AEC) activated acquisition for the three different phantom sizes and three tube voltages are summarized in Table 4. The table further tabulates the  $mAs_{QR}$  values which should be selected by the technologist to achieve the homogeneous image noise among the

phantoms at different kVp settings. In this study, it was presumed that images of adequate diagnostic quality are obtained on small, medium, and large-sized phantoms when scanned with standard scanning protocols, that is, 130 kV and 150  $mAs_{QR}$ . The mean values of image noise for the small, medium and large phantoms when scanned with standard scanning protocols were 7.8, 10.7 and 10.9 HU, respectively.

**Table 4:** Technical parameters and mean values of CT attenuation, image noise, and  $CTDI_{vol}$  for three different phantoms sizes at 300 mgI/MI

Exposure parameters		Small phantom (15 cm depth)			Medium phantom (20 cm depth)			Large phantom (24 cm depth)		
kV	$mAs_{QR}$	Mean CTA (HU)	Image noise(HU))	$CTDI_{vol}$ (mGy)	Mean CTA (HU)	Image noise (HU)	$CTDI_{vol}$ (mGy)	Mean CTA (HU)	Image noise (HU)	$CTDI_{vol}$ (mGy)
80	50	1064.3	23.3	1.4	1032.4	39.6	1.7	1020.5	56.0	1.9
80	100	997.5	16.2	2.9	1024.3	27.8	3.1	1014.1	34.4	3.6
80	150	998.1	13.8	4.0	1021.4	22.9	4.7	1006.1	26.1	5.8
80	200	996.4	11.0	5.3	1021.1	19.3	5.8	1009.4	22.5	7.4
80	250	997.3	7.9	6.6	1021.4	15.7	7.1	1008.4	21.2	9.0
110	50	674.2	11.7	2.6	682.7	22.0	2.9	678.0	23.9	3.4
110	100	674.8	8.5	5.0	681.6	15.7	5.6	671.6	17.8	6.9
110	150	673.8	7.9	7.6	681.9	11.0	8.3	671.7	13.0	10.4
110	200	673.0	6.1	11.3	681.5	9.8	12.8	668.9	11.4	15.0
110	250	673.8	5.4	13.0	681.3	9.3	14.2	669.5	10.2	17.9
130	50	554.5	8.3	3.6	558.5	15.5	3.9	545.6	18.8	4.7
130	100	555.4	8.1	6.9	557.0	12.9	7.6	546.8	11.4	9.5
130	150	555.4	7.8	10.2	558.6	10.7	11.5	544.1	10.9	14.1
130	200	555.5	5.1	14.1	556.87	7.7	16.6	546.4	8.4	20.0
130	250	553.9	4.6	18.6	557.43	7.4	20.0	545.7	7.6	24.5

By matching the image noise considered acceptable for the standard scan protocols, there was a 35.3% [(10.2–6.6 mGy)/10.2 mGy]

reduction in the  $CTDI_{vol}$  for the small-sized phantom when the technologist selected 80 kVp and 250  $mAs_{QR}$  exposure settings, instead

of standard scanning parameters of 130 kVp and 150 mAs<sub>QR</sub>. In the medium phantom, there was a 29.9% [(11.5–8.3 mGy)/11.5 mGy] reduction in the CTDI<sub>vol</sub> when the technologist selected the 110 kV and 150 mAs<sub>QR</sub> exposure settings, instead of standard scanning parameters of 130 kVp and 150 mAs<sub>QR</sub>. Unfortunately, it was not possible to reduce dose for the large phantom using low kVp technique (i.e., 80 kVp or 110 kVp) owing to the limitation in the selection of high mAs<sub>QR</sub> as the system was limited to a maximum of 300 mAs<sub>QR</sub>. For the same reason, further reduction of dose for the small and medium phantoms could not be attained. It should be noted that when the kVp was reduced to a lower value, the chosen mAs<sub>QR</sub> settings were approximately increased to offset the inherent increase in image noise. Hence, the images acquired at lower kVp settings maintained the image noise and presented better contrast compared with the original images obtained at the standard tube potential (130 kVp). Theoretically, lowering of the tube potential from 130 kVp to 80 kVp leads to reduction of dose by 70% at constant mA settings owing to the fact that radiation doses vary with a square of the tube voltages (Nagel et al. 2002). The less dose reduction of 35.3% compared with theoretical values was largely attributed to the use of higher mAs<sub>QR</sub> to achieve the acceptable image quality at a higher level to compensate for the increased image noise. Numerous studies have demonstrated the benefits of using the lower kVp settings in CTPA procedure. Szucs-Farkas et al. (2008) performed chest phantom study simulating thin, intermediate and thick patients. The employment of 80 kVp instead of 140 kVp resulted in a 44% reduction in CTDI<sub>vol</sub> for the thin phantom. Björkdahl and Nyman (2010) conducted phantom and patient study for diagnosis of pulmonary embolism at 100 and 120 kVp using 16-MDCT. The use of 100 kVp instead of 120 kVp resulted in a 38% reduction in CTDI<sub>vol</sub>. The utmost challenges for a low kVp technique for the MDCT angiography procedure have been appropriate patient selection. Further than a certain patient size,

very high mA values are needed for the low kVp to compensate the high image noise and to attain adequate diagnostic image quality (Hu et al. 2017). The high mA values required for the large patients are not practicable in the most of the cases.

On the other hand, higher concentrations of iodinated CM impart greater contrast enhancement compared with those of lower concentrations, which is mainly due to higher production of signal intensity on the detector. In the present study, the usage of highly concentrated iodinated CM (HU<sub>370</sub>) at lower kVp demonstrated higher contrast enhancement relatively to the lower (HU<sub>300</sub>) and moderate (HU<sub>350</sub>) concentrations. In spite of the fact that higher concentrations of iodinated CM improve contrast enhancement, but they result in an increased osmolality, which may cause higher radiological risks of contrast induced adverse reactions (Maddox 2002). Besides, the use of excessive concentrations of the iodinated CM can lead to beam hardening artifacts and directly degrade the image quality produced (Campbell et al. 2012).

In light of these observations and similar experience observed elsewhere (Papadakis et al. 2013), the use of low kVp and increase concentrations of iodinated CM based on patient size could substantially reduce patient dose from MDCT angiography procedures without markedly sacrificing image quality required for accurate diagnosis. These results suggest that there is a potential for reduction of radiation exposure in the small-sized adult and children patients on the basis of patient size through lowering the kVp settings and increase concentration of iodinated CM, while maintaining image quality required for accurate diagnosis. In view of the above, it is anticipated that the establishment of low kVp imaging protocols in MDCT will be an important step towards ensuring that unnecessary high doses to patients from CT are avoided, and that the resultant patient doses are reduced.

In spite of the fact that the study demonstrates that it is possible to minimize patient dose from MDCT angiographic

procedures through lowering kVp and increase concentrations of iodinated CM based on the patient sizes, the approach employed had a number of limitations. First, the CT scanning with low tube potential at 80 kVp was only conducted in a phantom study, and the phantom did not consider variability of body compositions, thus, whether these results are suitable to clinical applications need to be further confirmed. However, Björkdahl and Nyman (2010) demonstrated that a technique with 100 kVp could be used to improve the conspicuity of pulmonary arteries, while substantially decreasing patient dose. Second, the image quality was evaluated only on the basis of objective quality measures. A subjective evaluation of the image quality from experienced radiologists would add useful inputs towards optimization of the protocols used in this study. Third, the results presented in this study refer to 16-slice MDCT scanner of a single manufacturer and that the AEC system investigated in this study is based on the image quality reference mAs concept. It would be interested to apply the methodology presented in this study to different scanners with a higher number of detector rows and with AEC systems, which embody the noise index concept for mA modulation.

### Conclusions

The rationale of lowering the X-ray tube potential while increasing concentrations of iodinated contrast materials to patients undergoing CTPA procedure based on patient size was demonstrated. The phantom studies demonstrated that in comparison with 130 kVp, regardless of the selected mAs or quality reference tube current-time product, images obtained at 80 kVp and 110 kVp showed 76.2% to 99% and 19% to 26% enhancement in CT attenuation of iodinated contrast material, respectively. This study also demonstrated that CNR was substantially improved when tube potential setting and iodine concentrations were increased. The phantom studies further demonstrated that radiation dose to the small-sized phantom could be reduced up to 35.3%

with the use of 80 kVp instead of 130 kVp, while in the medium-sized phantom could be reduced up 29.9% with the use 110 kVp instead of 130 kVp without degradation of diagnostic image quality. In light of the above, lowering tube potential and increase concentration of iodinated CM could significantly reduce radiation doses to small-sized adult and children patients undergoing CTPA procedure without impairing image quality. Based on the data presented and the limitations in this study, further studies are recommended to adequately transfer the phantom studies to the clinical studies, which may involve diagnostic and clinical factors and hence introduce patient size specific protocols for various MDCT angiography studies to medical CT centres.

### Acknowledgments

The authors sincerely thank the owners of the Besta Diagnostic Centre for allowing them to use their CT facility. Similarly, they thank Dr. M. Maboko, Mr. K. Khalid and Ms. J. Kangati for their valuable technical support at the MDCT facility. Authors are also grateful to the National Institute for Medical Research for approval of the research proposal.

### Funding

This study was financially supported by the Tanzania Commission for Science and Technology.

### References

- Aschoff AJ, Catalano C, Kirchin MA, Krix M, and Albrecht T 2017 Low radiation dose in computed tomography: the role of iodine. *Br. J. Radiol.* 90: 20170079.
- Björkdahl P and Nyman U 2010 Using 100-kVp instead of 120-kVp computed tomography to diagnose pulmonary embolism almost halves the radiation dose with preserved diagnostic quality. *Acta Radiol.* 51(3): 260-270.
- Campbell C, Lubner MG, Hinshaw JL, del Rio AM, Brace CL 2012 Contrast media-doped hydrodissection during thermal ablation: optimizing contrast media concentration for improved visibility on CT images. *Am J Roentgenol.* 199: 677-682.

- Goo HW 2012 CT Radiation dose optimization and estimation: An update for radiologists. *Korean J. Radiol.* 13(1): 1-11.
- Gupta AK, Nelson RC, Johnson GA, Paulson EK, Delong DM and Yoshizumi TT 2003 Optimization of eight-element multi-detector row helical CT technology for evaluation of the abdomen. *Radiology* 227: 739-745.
- Hausleiter J, Meyer T, Hermann F, Hadamitzky M, Krebs M, Gerber TC, McCollough C, Martinoff S, Kastrati A, Schömig A, Achenbach S 2009 Estimated radiation dose associated with cardiac CT angiography. *JAMA.* 301(5): 500-507.
- Hu X, Ma L, Zhang J, Li Z, Shen Y and Hu D 2017 Use of pulmonary CT angiography with low tube voltage and low-iodine-concentration contrast agent to diagnose pulmonary embolism. *Sci. Rep.* 7: 12741.
- IPEM (Institute of Physics and Engineering in Medicine) 2005 Recommended standard for the routine performance testing of diagnostic X-ray imaging systems. Reports No. 77. York: IPEM.
- Ma Y, Zhang H, Zhang Y, and Yu T 2017 A study on CT pulmonary angiography at low kV and low-concentration contrast medium using iterative reconstruction. *Biomed. Res.* 28(17): 7683-7687.
- Maddox TG 2002 Adverse reactions to contrast materials: recognition, prevention, and treatment. *Am. Fam. Physician* 66: 1229-1234.
- Moynihan WA, Bowden L, Kiely P and O'Brien JM 2017 A comparison of 100 kVp versus 120 kVp CTPA acquisition with direct comparisons of test bolus and bolus tracking at same and different voltages in a multidetector 64 slice CT scanner. *Int. J. Radiol. Radiat. Ther.* 4(2): 363-368.
- Nagel HD, Galanski M, Hidajar N, Maier W, Schmidt T 2002 Radiation exposure in computed tomography. Fundamentals, influencing parameters, dose assessment, optimization, scanner data, terminology, Hamburg: CTB Publications, 2002.
- Ngaile JE, Msaki P and Kazema R 2012 Patient-size-dependent radiation dose optimization technique for abdominal CT examinations. *Radiat. Prot. Dosim.* 148: 189-201.
- Nyman U, Björkdahl P, Olsson ML, Gunnarsson M and Goldman B 2012 Low-dose radiation with 80-kVp computed tomography to diagnose pulmonary embolism: a feasibility study. *Acta Radiol.* 53: 1004-1013.
- Papadakis AE, Perisinakis K, Raissaki M and Damilakis J 2013 Effect of X-ray tube parameters and iodine concentration on image quality and radiation dose in cerebral pediatric and adult CT angiography: a phantom study. *Investig. Radiol.* 48(4): 192-199.
- Razak HRA, Rahmat SMSS and Saad WMM 2013 Effects of different tube potentials and iodine concentrations on image enhancement, contrast-to-noise ratio and noise in micro-CT images: a phantom study. *Quant. Imaging Med. Surg.* 3(5): 256-261.
- Schindera ST, Tock I, Marin D, Nelson RC, Raupach R, Hagemeister M, von Allmen G, Vock P and Szucs-Farkas Z 2010 Effect of beam hardening on arterial enhancement in thoracoabdominal CT angiography with increasing patient size: An in vitro and in vivo study. *Radiology* 256(2): 528-535.
- Schindera ST, Winklehner A, Alkadhi H, Goetti R, Fischer M, Gnannt R and Szucs-Farkas Z 2013 Effect of automatic tube voltage selection on image quality and radiation dose in abdominal CT angiography of various body sizes: a phantom study. *Clin. Radiol.* 68 (2): e79-e86.
- Sun Z and Ng KH 2010 Multislice CT angiography in cardiac imaging. Part III: radiation risk and dose reduction. *Singapore Med. J.* 51(5): 374-380.
- Szucs-Farkas Z, Verdun FR, von Allmen G, Mini RL, and Vock P 2008 Effect of X-ray tube parameters, iodine concentration, and patient size on image quality in pulmonary computed tomography angiography: a chest-phantom study. *Investig. Radiol.* 43(6): 374-381.